Environmental versus biomineralization controls on the intratest variation in the trace element composition of the planktonic foraminifera *G. inflata* and *G. scitula*

Ed C. Hathorne,[1,2,3] Rachael H. James,[1,4] and Richard S. Lampitt[5]

[1]   The intratest variation in the chemical composition of *Globorotalia scitula* and *G. inflata* recovered from a sediment trap sample collected at 3000 m in the North Atlantic in early spring has been investigated using laser ablation inductively coupled plasma–mass spectrometry and electron microprobe. Mg/Ca, Li/Ca, B/Ca, Mn/Ca, and Ba/Ca vary by up to a factor of 10 through the test walls. Water column properties, including temperature and salinity, are well documented at the trap site, and the observed variations are too large to be explained by vertical migration of the foraminifera. However, changes in calcite precipitation rate, crystal structure, or the chemical composition of the internal calcification reservoir also cannot, by themselves, fully account for the pattern of intratest variability. Nevertheless, the average Mg/Ca for each chamber generally produces a Mg/Ca temperature that matches that measured in the water column. The exception is small, morphologically distinct *G. inflata* tests that have anomalously high Mg/Ca.

1.   Introduction

[2]   The trace element chemistry of the calcite shells (tests) of planktonic foraminifera records an abundance of information about the environment in which the test grew. For this reason, fossilized tests are a key tool in paleoceanography and have been used to reconstruct seawater temperature [e.g., *Nürnberg et al.*, 1996; *Lea et al.*, 1999; *Rosenthal et al.*, 2000; *Lear et al.*, 2000; *McConnell and Thunell*, 2005] as well as other environmental parameters including carbonate chemistry [e.g., *Russell et al.*, 2004; *Yu et al.*, 2007], nutrient utilization [*Elderfield and Rickaby*, 2000] and trace element concentrations [e.g., *Hathorne and James*, 2006]. Nevertheless, calibrating the relationship between test chemistry and an environmental variable remains fraught with difficulty because foraminiferal calcite is precipitated under tight biological control by the organism [e.g., *Hemleben et al.*, 1989; *Bentov and Erez*, 2005]. There is commonly an offset (known as the "vital effect") between the chemical composition of biogenic and inorganic calcite [e.g., *Elderfield et al.*, 1996; *Erez*, 2003] and this is difficult to quantify because the size of the vital effect tends to vary not only with species [e.g., *Hathorne and James*, 2006], but also with the size of the test [*Elderfield et*

al., 2002; *Ni et al.*, 2007]. Thus, the effects of biomineralization processes on test chemistry, and their implications for the reconstruction of past environmental parameters, need to be properly understood.

[3]   One way to obtain information about biomineralization processes is by measurement of the variability of trace elements *within* a foraminiferal test [*Brown and Elderfield*, 1996; *Eggins et al.*, 2003; *Hathorne et al.*, 2003; *Erez*, 2003; *Eggins et al.*, 2004; *Gehlen et al.*, 2004; *Sadekov et al.*, 2005; *Anand and Elderfield*, 2005; *Kunioka et al.*, 2006; *Sadekov et al.*, 2008; *Tachikawa et al.*, 2008]. New microanalytical techniques, such as nanoSIMS [*Kunioka et al.*, 2006] and laser ablation inductively coupled plasma–mass spectrometry (ICP-MS) [e.g., *Eggins et al.*, 2003; *Hathorne et al.*, 2003], now allow accurate and precise measurement of low levels of a number of elements at high (μm) resolution. Techniques such as these have, for example, identified a layer of high Mg/Ca calcite intimately associated with the primary organic membrane [*Kunioka et al.*, 2006], while other studies have shown that the chemistry of gametogenic calcite is distinct from that of inner (chamber) calcite [e.g., *Brown and Elderfield*, 1996; *Eggins et al.*, 2003; *Hathorne et al.*, 2003].

[4]   Despite these advances, the relative effects of biomineralization versus environmental controls on the intratest variability in trace elements remain uncertain. Some studies suggest that variations in Mg/Ca can simply be attributed to calcite precipitation at variable water depth (and hence variable temperature and seawater chemistry) because of the vertical migration of foraminifera through the water column [*Brown and Elderfield*, 1996; *Eggins et al.*, 2003]. However, more recent reports suggest that this explanation is incorrect because the range in Mg/Ca (from

---

[1]Department of Earth Sciences, Open University, Milton Keynes, UK.
[2]Center for Marine Environmental Sciences, University of Bremen, Bremen, Germany.
[3]Now at Leibniz Institute of Marine Sciences at University of Kiel (IFM-GEOMAR), Kiel, Germany.
[4]Now at National Oceanography Centre, Southampton, UK.
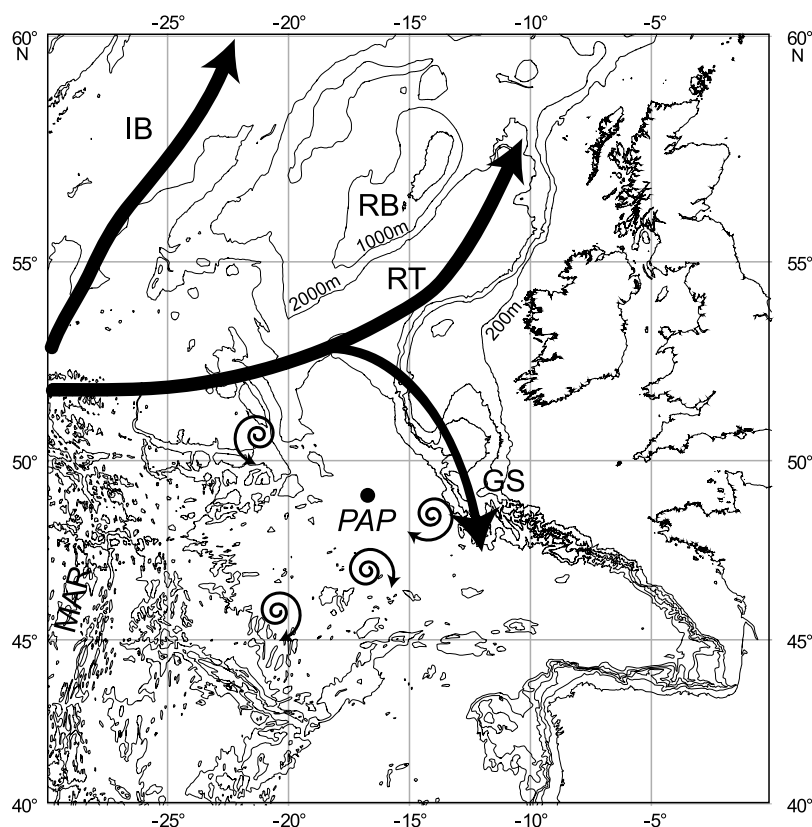[5]National Oceanography Centre, Southampton, UK.

Figure 1. Location of the PAP site with bathymetry and generalized circulation of the region. The polar front is located in the region of the arrow in the top left corner of the map (also see Figure S1). Arrows represent the North Atlantic current system, and spirals show the positions of some documented eddies. MAR, Mid-Atlantic Ridge; IB, Iceland Basin; RB, Rockall Bank; RT, Rockall Trough; GS, Goban Spur.

~1 to >10 mmol/mol) is too large [*Eggins et al.*, 2004; *Sadekov et al.*, 2005; *Anand and Elderfield*, 2005; *Kunioka et al.*, 2006]. What is also unclear is why the range in Sr/Ca values is small relative to other elements [*Eggins et al.*, 2003; *Anand and Elderfield*, 2005].

[5] The two foraminifera species studied here, *G. inflata* and *G. scitula,* are of considerable interest to paleoceanographers because they provide records of environmental variables in the thermocline and intermediate water masses [*Ortiz et al.*, 1996; *Itou et al.*, 2001; *Chiessi et al.*, 2007; *Cléroux et al.*, 2007, 2008]. *G. inflata* is a nonspinose species and oxygen isotope studies indicate that it lives at depths of between 50 and 500 m [*Fairbanks et al.*, 1980; *Erez and Honjo*, 1981], although it tends to calcify over a narrower depth range depending on the local hydrography [*Wilke et al.*, 2006; *Chiessi et al.*, 2007]. Its depth habitat is also affected by food availability; the abundance of *G. inflata* tracks fluorescence [*Lončarić et al.*, 2006] and nutrient distributions [*Cléroux et al.*, 2007]. *G. inflata* is mostly considered symbiont barren [*Ortiz et al.*, 1996; *Wilke et al.*, 2006; *Yu et al.*, 2007], but has occasionally been observed to contain chrysophyte photosymbionts [*Hemleben et al.*, 1989]. *G. scitula* is also a nonspinose species and has a depth habitat of between 100 and >1000 m depending on seasonal hydrography [*Itou et al.*, 2001]. A study from the northeastern North Atlantic found that *G. scitula* is most abundant in the upper part of the mesopelagic zone (above 700 m but below the euphotic zone) [*Schiebel et al.*, 1995].

[6] The aim of this study is to better constrain environmental versus biomineralization controls on the intratest variability in the chemical composition of foraminifera. To this end, we present the results of analyses of *G. inflata* and *G. scitula* that were recovered from a sediment trap over a 2 week period for which the environmental parameters in the water column are well established. We utilize the multielement capability of laser ablation ICP-MS and the high spatial resolution of electron microprobe mapping to reveal the intratest heterogeneity of trace elements. We demonstrate that, for most elements, the environmental control is relatively small, and we then go on to assess a number of proposed models for biomineralization, to see whether they can account for the variations that we observe.

2. Methods

2.1. Oceanographic Setting

[7] The Porcupine Abyssal Plain (PAP) sediment trap mooring is located in the northeast Atlantic Ocean in the region of 48°50N, 16°30W in ~4800 m water depth [*Lampitt et al.*, 2001] (Figure 1) and has been occupied since 1989 (http://www.noc.soton.ac.uk/pap). The region is characterized by sluggish surface water flow and lies to the
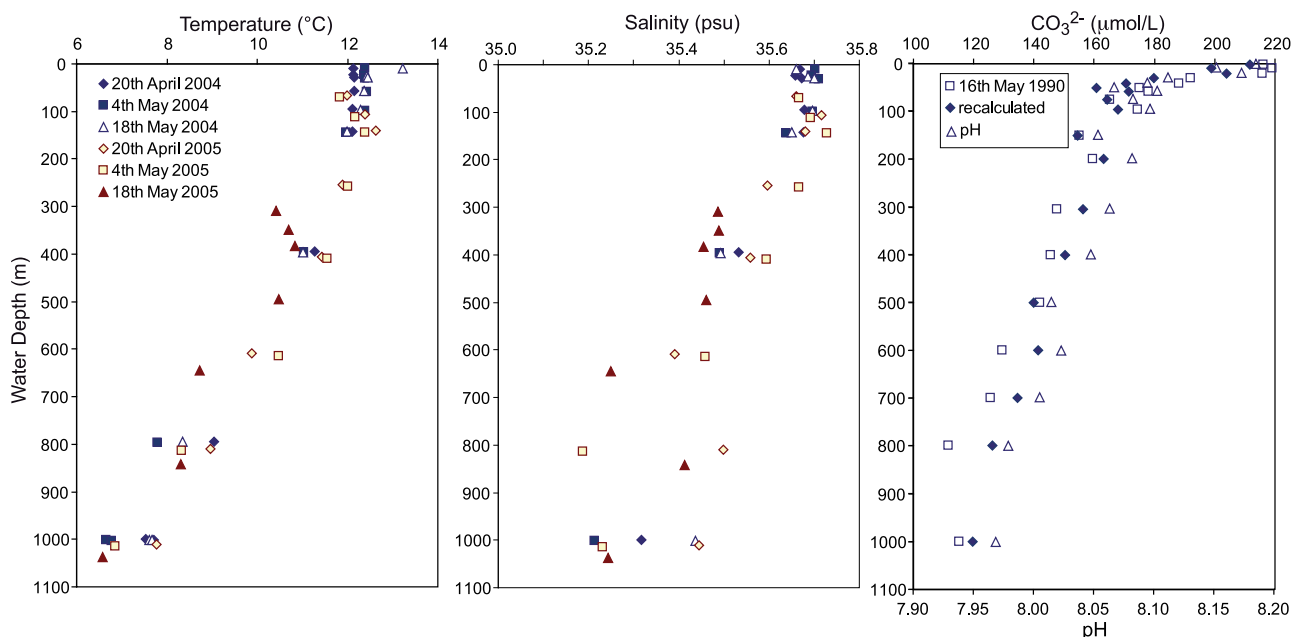
Figure 2. Temperature and salinity of the upper water column at the PAP sediment trap site (http://www.noc.soton.ac.uk/pap). Also shown are pH and carbonate ion concentration profiles calculated from measurements made at a nearby site in May 1990 [*Rommets*, 2003; *Rommets et al.*, 1991, 2003] using the CO2sys macro [*Pierrot et al.*, 2006].

southeast of the main North Atlantic Current (NAC) and well to the north of the subtropical gyre [*Pingree*, 1993] (Figure 1). Circulation at the depth of the thermocline in the region is also weak [*Bower et al.*, 2002]. Cyclonic and anticyclonic eddies have been observed in this area [e.g., *Pingree and Le Cann*, 1991] but the eddy kinetic energy in the PAP region is low (~100 cm²/s²) [*Heywood et al.*, 1994; *Fratantoni*, 2001; *Stammer et al.*, 2006]. Eddies have been observed to form at the subpolar front (Figure 1) [*Mittelstaedt*, 1987]; these are generally composed of proximal water masses [*Harvey and Glynn*, 1985; *Robinson et al.*, 1993] but entrainment of warm salty Mediterranean Water (MW) at depth has been documented [*Harvey and Glynn*, 1985; *Mittelstaedt*, 1987]. *Schauer* [1989] describes a cyclonic eddy with a deep MW core in the PAP region while *Shoosmith et al.* [2005] document "meddy-like" anticyclones with MW cores. Other eddies in the region have been observed to remain almost stationary for months [*Pingree and Le Cann*, 1991].

[8] Eddies act to shoal or deepen isopycnals and in the PAP region they can cause a reduction in water temperature of 2°C, or less, at a depth of 200 m [*Mittelstaedt*, 1987; *Robinson et al.*, 1993]. Mediterranean Water has only been observed at depths of > 500 m [e.g., *Schauer*, 1989; *Shoosmith et al.*, 2005]. Shoaling isopycnals and eddy-wind interactions cause upwelling of nutrient rich waters, which increases productivity and changes plankton communities [e.g., *Lochte and Pfannkuche*, 1987; *Woodward and Rees*, 2001; *McGillicuddy et al.*, 2007]. However, meteorological conditions generally have the greatest influence on surface water temperatures [*Pingree and Le Cann*, 1991] and storms can dramatically increase the mixed layer depth, increasing

the level of nutrients and chlorophyll *a* [*Schiebel et al.*, 1995].

2.2. Sampling

[9] The sediment trap mooring was deployed at about 49°N, 16°30W from 8 April 2001 to 24 February 2002. Time series sediment traps (Parflux with 21 sample cups) [*Honjo and Doherty*, 1988] of mouth area 0.5 m² were positioned at a depth of about 3000 m which is about 1800 m above the seabed and hence well clear of locally resuspended sediment. Sample cups were prefilled with hypersaline buffered formalin [*Lampitt et al.*, 2000]. Collection periods varied from 2 to 8 weeks depending on the time of year and hence the expected rate of change in flux with time. The JGOFS protocol (SCOR 1990) was adopted for sample handling and is further described by *Newton et al.* [1994]. Swimmers were removed by hand under a dissecting microscope.

[10] The sample cup which was open during the period 6−20 May was selected and two species of planktonic foraminifera (*Globorotalia inflata* and *Globorotalia scitula*) were picked from the collected material. This was during the early spring bloom just prior to a period of particularly high downward flux (Figure S2) and, in terms of foraminifera, the sample is dominated by large *G. inflata* tests.[1] None of the tests contained a significant amount of cytoplasm, which suggests that the foraminifera had undergone gametogenesis. Sediment traps potentially collect particles from large distances away from their mooring because of horizontal advection. Even though the PAP site is located in

---

[1]Auxiliary materials are available in the HTML. doi:10.1029/2009PA001742.
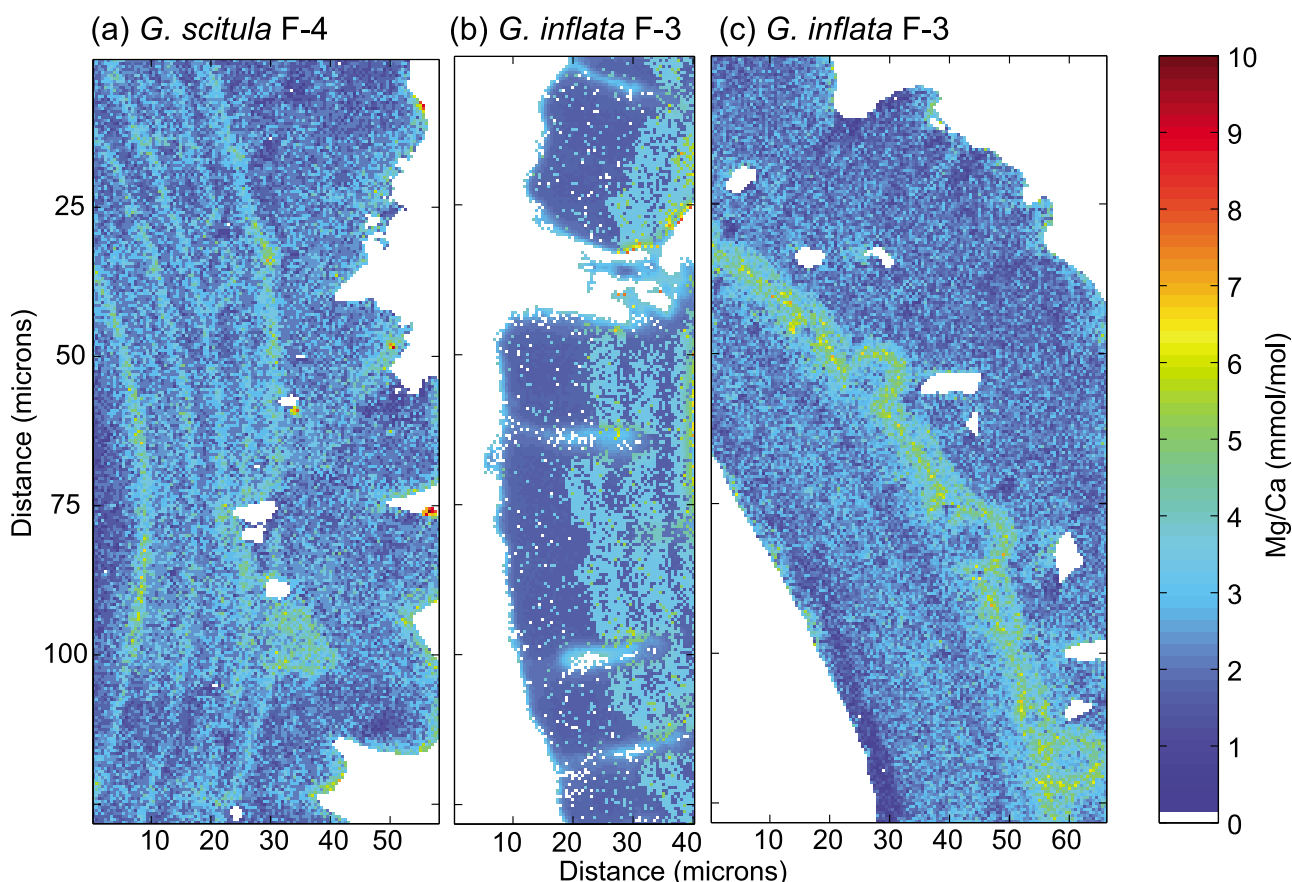
Figure 3. (a−c) Electron microprobe Mg/Ca maps across test wall cross sections. Areas with Ca counts <40% of the maximum value are blanked out (shown in white) as these are affected by edge effects. The outer part of the test wall is shown on the right-hand side of Figures 3a and 3c and on the left-hand side of Figure 3b.

a region of low kinetic energy, the material collected at 3000 m is likely to have originated from an area around the mooring with a radius of 200 km [*Lampitt et al.*, 2001]. However, large planktonic foraminifera shells (>400 μm) such as those used in this study sink at speeds of between 1500 and 750 m/d [*Takahashi and Bé*, 1984] so the sampling length scale is only 20–40 km [*Siegel and Deuser*, 1997]. Since 2002, temperature and salinity profiles have been continuously recorded for the upper 1000 m of the water column at PAP using in situ MicroCAT sensors. Typical profiles, for the time period over which the foraminifera are thought to have calcified (the 4 weeks prior to collection), are shown in Figure 2. Profiles of pH and carbonate ion concentration [CO_3^{2-}] calculated from measurements at a nearby site are also shown. Note that there is little interannual variability in temperature and salinity in the upper part of the water column (where calcification takes place) at this time of year. Salinity shows more variability below ~600 m, probably because of eddy activity.

2.3. Sample Preparation

[11] A portion of the sediment trap material was wet sieved through a 63 μm mesh, placed on filter paper, and dried in an oven at 45°C. Individual foraminifera were hand picked and placed into 0.5 ml microcentrifuge vials. Oxidative cleaning to remove organic material was performed either with buffered hydrogen peroxide [after *Barker et al.*, 2003] or by soaking in ~10% sodium hypochlorite for 24 h. After leaching, the sample was ultrasonicated for 1 min and then rinsed 5 times with Milli-Q water. The sample was then transferred in Milli-Q water onto a clean plastic microfossil slide and allowed to dry. For laser ablation ICP-MS analyses, the larger foraminifera tests (>438 μm) were mounted onto a double-sided carbon adhesive disk using a clean dry brush.

2.4. Laser Ablation ICP-MS

[12] Laser ablation ICP-MS analyses were conducted at the Open University using a 193 nm excimer laser ablation system (New Wave Research) coupled to a quadrupole ICP-MS (Agilent 7500 series). Profiles of the variation in chemical composition through the wall of a foraminifera test were obtained by targeting either a 70 or 100 μm diameter spot on the test surface, ablating through the test wall, and stopping the laser when the wall was penetrated. Ablations were conducted with a laser power of ~3 J/cm^2 and a repetition rate of 5 Hz; under theses conditions it typically took 30 s or longer to ablate through the test wall.
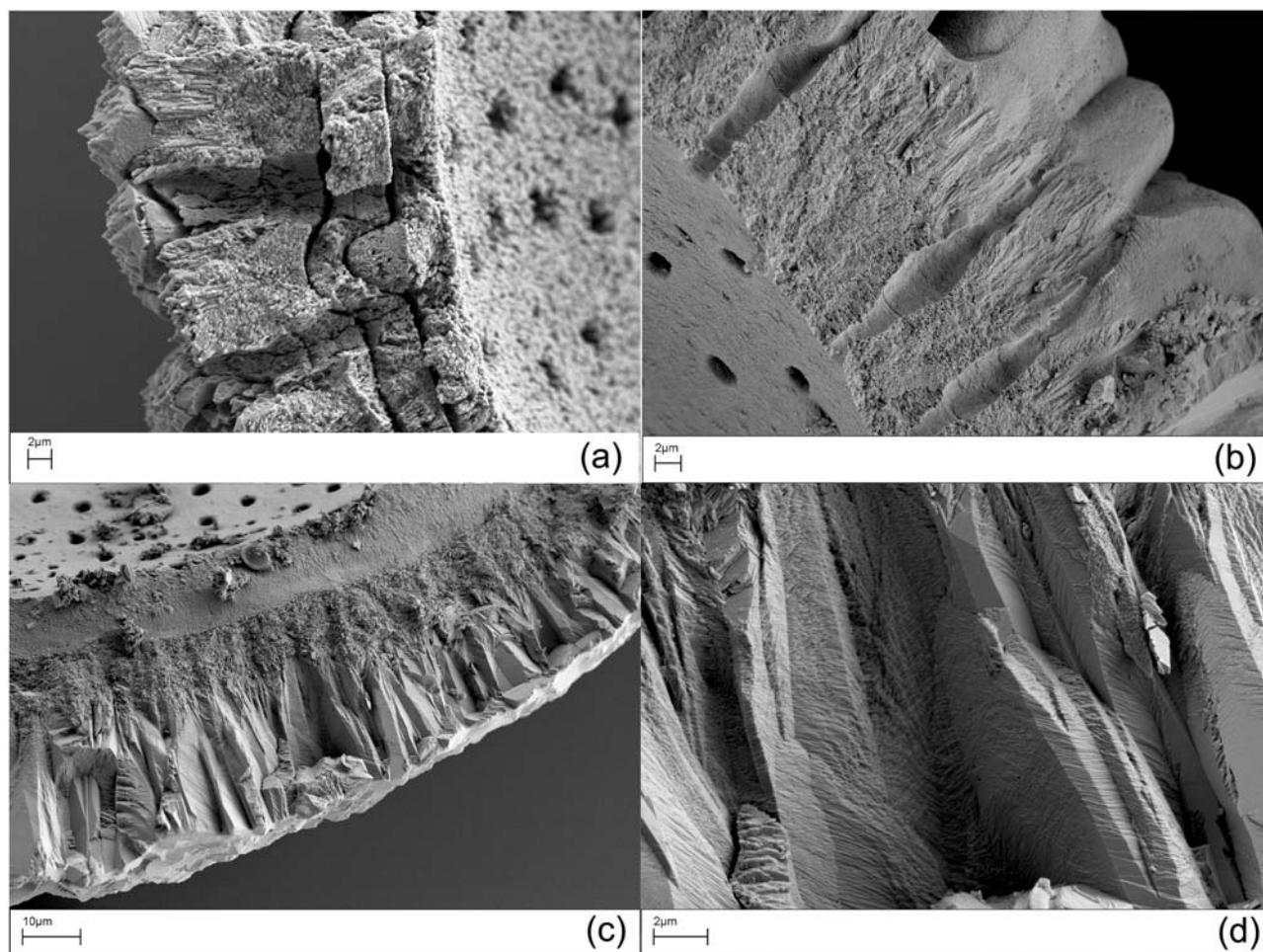
Figure 4. Scanning electron microscope images of test wall cross sections: (a) *G. bulloides* etched by reductive cleaning, (b) *G. inflata* used in this study, (c) *G. scitula* used in this study, and (d) detail of Figure 4c.

First, the gas blank was measured during which the laser beam is blocked by a shutter. The shutter was then removed, the sample ablated the transient signals from the analyte were then collected for the ablation period. Data were acquired for [7]Li, [11]B, [24]Mg, [25]Mg, ^{31}P, [34]S, [43]Ca, [44]Ca, [47]Ti, [55]Mn, [65]Cu, [66]Zn, [88]Sr, [90]Zr, [137]Ba, and [238]U. Raw counts were processed offline using standard spreadsheet software and element/Ca ratios were determined via the method of *Rosenthal et al.* [1999] using [43]Ca as the internal standard. Analyses were calibrated using the COCAL calcite and NIST 612 glass standards [*Hathorne et al.*, 2008]. In this study the ICP-MS was tuned to give the best sensitivity for the low mass elements so many of the higher mass elements were below the detection limit of the technique. For this reason, only data for Li/Ca, B/Ca, Mg/Ca, Mn/Ca, Sr/Ca and Ba/Ca are presented here. The reproducibility of this depth profiling technique is generally ~10% (1σ), determined by repeat analysis of the JCp-1 coral reference material (Figure S3).

2.5. Electron Microprobe

[13] After laser ablation ICP-MS analysis the samples were gold coated and imaged with a Scanning Electron Microscope (SEM). The samples were then vacuum impregnated with epoxy resin (Struers Epofix) to form a 25 mm diameter round block, ground to reveal a cross section through the wall of the test and polished to produce a smooth surface. The block was then carbon coated for Electron Microprobe (EMP) analysis. Maps of the distribution of Mg and Ca were obtained using a 20 kV and 20 nA beam focused to a 1 μm spot. The stage was moved 0.5 μm between pixels and the dwell time per pixel was 500 ms. Raw intensity ratios were calibrated using a carbonatite calcite crystal (OKA) that has Mg/Ca = 4.5 mmol/mol [*Hathorne et al.*, 2008].

3. Results

[14] Electron microprobe maps (Figure 3) of test wall cross sections reveal that Mg/Ca varies from <1 mmol/mol (the approximate detection limit of the technique) to ~6 mmol/mol. The outermost part of the test has lower Mg/Ca than the inner part of the test, and a thin, ~3 μm wide layer with highest Mg/Ca generally lies between the two (this is seen most clearly in Figure 3c). The maps also show that additional thin layers with very high Mg/Ca can
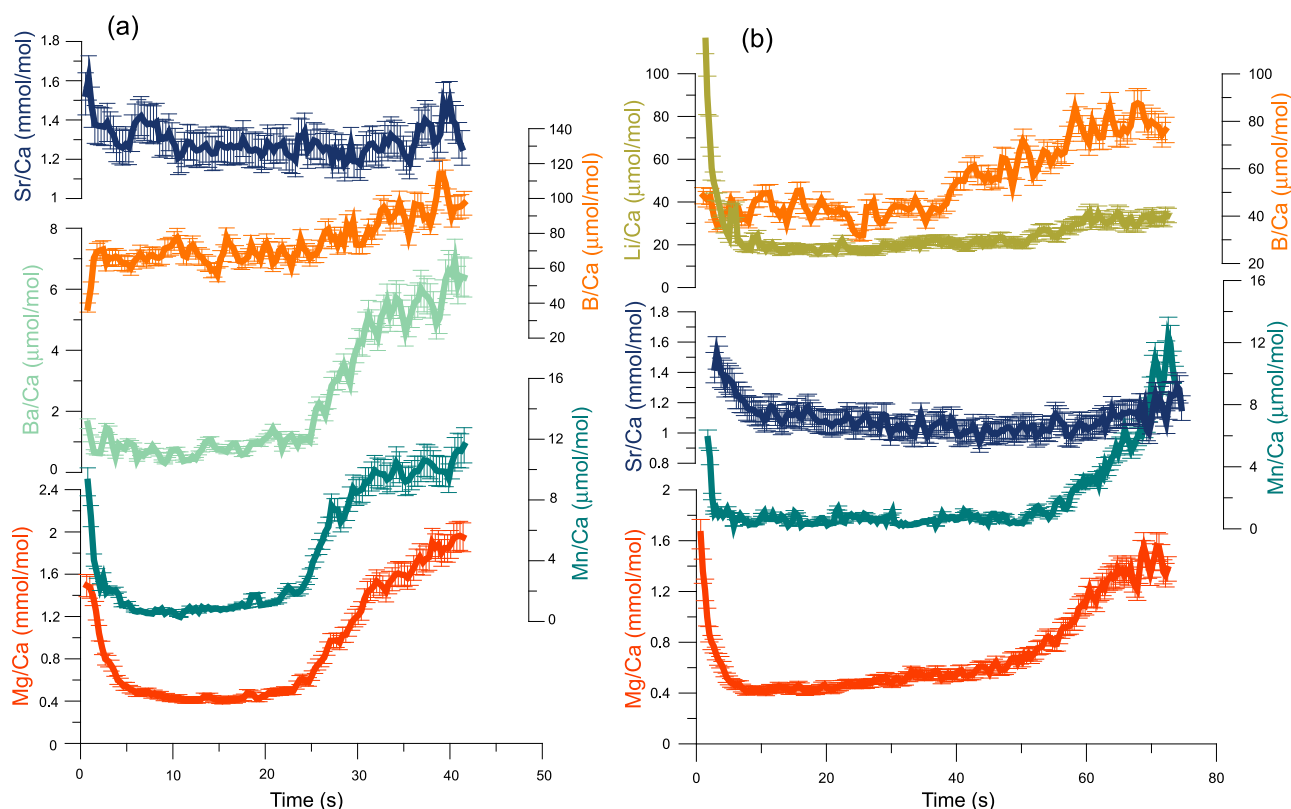
Figure 5. Laser ablation ICP-MS profiles of trace element/Ca through the test walls of (a) *G. inflata* and (b) *G. scitula*. All analyses were conducted by ablating from the outside of the test toward the inside. Error bars show the reproducibility of measurements of a standard powder pellet (see Figure S3).

exist within the inner (high Mg/Ca) layer. This probably reflects calcite that has been added as a new chamber forms [*Bé et al.*, 1979]. These bands are not present in the outermost low Mg/Ca calcite; the outermost layer thus probably represents the gametogenic crust [e.g., *Bé*, 1980; *Caron et al.*, 1990]. Crucially, the outermost layer has a distinct crystal structure with large elongate euhedral crystals; by contrast, the inner calcite layer consists of much smaller (submicron) crystallites (Figure 4).

[15] Laser ablation analyses (Figures 5 and 6) reveal the presence of a surface veneer that is enriched in all trace elements (with the exception of B) relative to Ca. High levels of Mg/Ca at the test surface are also apparent in the EMP maps, but this could be due to "edge artifacts" associated with this technique [*Eggins et al.*, 2004]; such artifacts are not an issue with laser ablation [*Hathorne et al.*, 2008]. Like the EMP maps, the laser ablation profiles show that the outer part of the test has lower Mg/Ca than the inner part. However, mixing of sample during transport from the laser ablation chamber to the ICP-MS means that the overall range in Mg/Ca is less than that measured by EMP. For the same reason, the thin layers with highest Mg/Ca are not resolved. However, the key advantage of laser ablation ICP-MS is that it is much more sensitive, and it is thus possible to measure the variation of Li/Ca, B/Ca, Mn/Ca and Ba/Ca through the test wall; this proves to be similar to that recorded for Mg/Ca. This contrasts with Sr/Ca which displays little

variability across the test wall. Plots of Li/Ca, B/Ca, Mn/Ca and Ba/Ca versus Mg/Ca display a positive relationship (Figure 7) but there are generally two distinct quasi-linear trends implying mixing of three components. In each case one trend is defined by the first few seconds of ablation and so represents mixing between the trace element rich surface veneer and the outermost calcite layer (Figures 7a–7c). The other trend represents mixing of the outermost calcite layer with the inner calcite layer and for this trend the correlation between Mg/Ca and element/Ca tends to be strong. Mn/Ca and Ba/Ca versus Mg/Ca give average r^2 values of 0.84 and 0.83, respectively. The correlation between Li/Ca and Mg/Ca is slightly weaker (r^2 = 0.76) while the correlation between B/Ca and Mg/Ca is variable (r^2 ranges from 0.83 to 0.30 (Figures 7d and 7e)). Finally, Sr/Ca is not significantly ($p < 0.05$) correlated with Mg/Ca (Figure 7f).

[16] The gradient of the lines that link element/Ca with Mg/Ca (excluding the first few seconds of ablation) is distinctly different between the two species; *G. scitula* has significantly higher gradients than *G. inflata* (Table 1). Because the highest Mg/Ca values observed in the microprobe maps are not resolved by the laser ablation analyses (because of signal mixing), it follows that the true range of other element/Ca ratios is also not recorded. If the relationships documented in Table 1 and Figure 7 are extrapolated to the highest Mg/Ca values observed in the microprobe maps, then the range of Mn/Ca and Ba/Ca values agrees
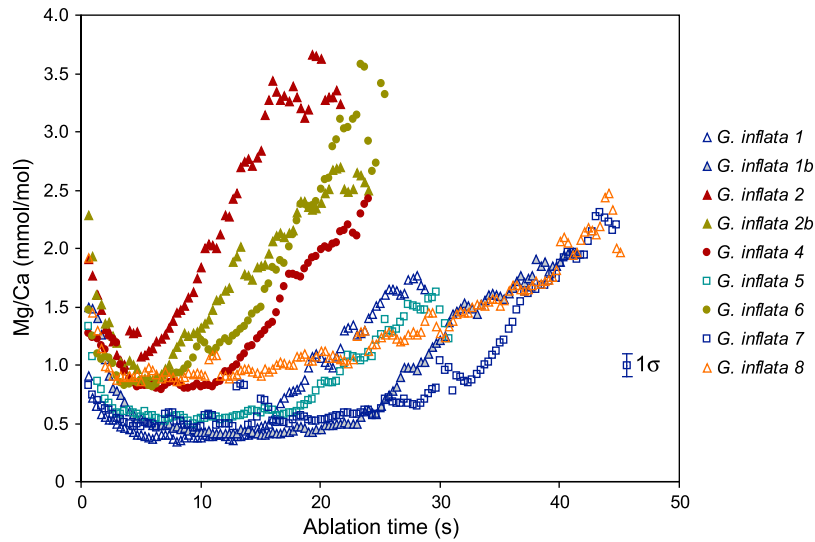
Figure 6. Laser ablation ICP-MS profiles of Mg/Ca through the test walls of *G. inflata*. Analyses of smaller tests with only 3–3.5 chambers in the final whorl are shown by solid symbols. Open symbols represent larger tests that have 4 chambers in the final whorl.
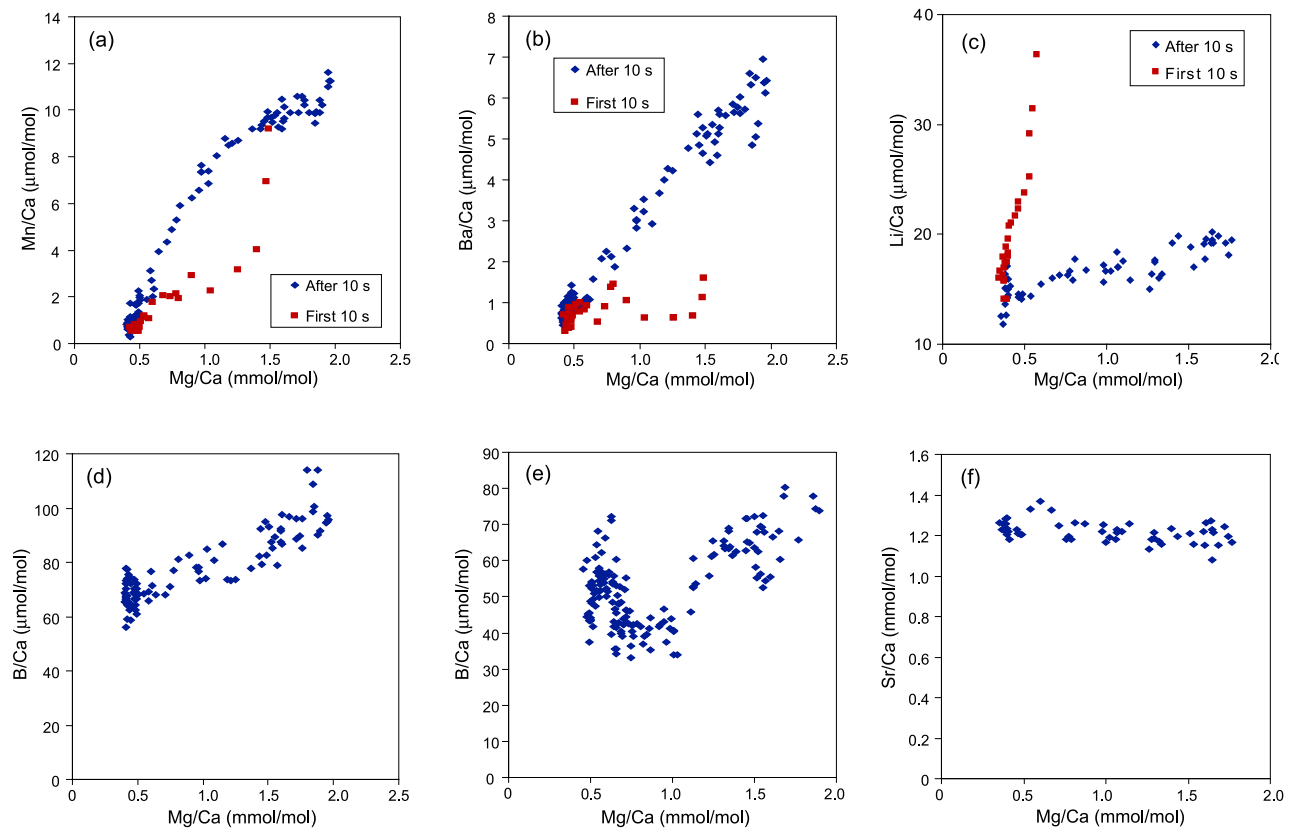
Figure 7. (a, b, c, d, and f) Relationship between trace element/Ca ratios and Mg/Ca ratios through *G. inflata* test walls. (e) Same as other plots but for a *G. scitula* test. The first 10 s of analysis represents mixing between the surface veneer and outer calcite for Mn, Ba, and Li (Figures 7a–7c). The remaining data result from mixing of inner and outer calcite layers, with the exception of B (Figures 7d and 7e), which shows more complex behavior, and Sr (Figure 7f), which does not vary with Mg/Ca (at the $p < 0.005$ level). See Table 1 for a summary of the data obtained for all tests.

Table 1. Average Gradient and Standard Deviation of Lines Defining the Relationship Between Element/Ca and Mg/Ca for Each of the Individual *G. inflata* and *G. scitula* Tests That Were Recovered From the Sediment Trap[a]

	Li/Ca		B/Ca		Mn/Ca		Ba/Ca	
	Gradient	σ	Gradient	σ	Gradient	σ	Gradient	σ
G. inflata	5.2×10^3	2.8×10^3	18.3×10^3	9.4×10^3	3.4×10^3	2.5×10^3	2.3×10^3	1.2×10^3
G. scitula	30.5×10^3	17.3×10^3	54.5×10^3	24.0×10^3	10.0×10^3	4.1×10^3	9.0×10^3	2.8×10^3

[a]Here σ, standard deviation. For *G. inflata* n = 8, and for *G. scitula* n = 2. Note that data for the first 10 s of each analysis are excluded (see text for details). For B/Ca, only analyses showing significant (p < 0.05) relationships are considered.

well with those measured in a recent nanoSIMS study [*Kunioka et al.*, 2006].

4. Discussion

4.1. Surface Veneer

[17] Our analyses reveal that all of the foraminifera tests have a surface veneer that is enriched in all trace elements, except B. Enrichment of trace elements at the test surface has previously been observed for core top specimens [*Eggins et al.*, 2003; *Hathorne et al.*, 2003; *Kunioka et al.*, 2006] but these new data for tests that have never reached the sediments suggest that the surface veneer could be an original part of the test. The possibility remains that the surface coating formed either in the water column or after the test settled in the sediment trap (for example, by adsorption from clays), but high concentrations of trace elements at the test surface have also been reported for plankton tow samples [*Eggins et al.*, 2003] indicating that they are present even in live specimens. Additionally, ablation of only the very surface of the test produces a similar number of counts for Ca as ablation of the calcite standard (Figure S4). This raises the possibility that the surface veneer is a Ca-rich phase, possibly biogenic amorphous calcium carbonate, as has been observed for other calcite mineralizing organisms [e.g., *Addadi et al.*, 2003].

4.2. Intratest Variation in the Trace Element Composition of Planktonic Foraminifera

[18] Recent work has suggested that highest Mg/Ca layers are associated with organic components of the test [*Kunioka et al.*, 2006]. Here we find that the shape of the layer with highest Mg/Ca mimics the arrangement of the calcite crystals sometimes revealed by test cleaning (Figure 4a). Additionally, the tests in this study were cleaned of organic material and no difference was observed between the two cleaning techniques. Thus, we conclude that the layer with highest Mg/Ca is calcite located adjacent to the primary organic membrane, rather than the organic membrane itself. Bands of high Mg/Ca have been previously described for symbiont bearing species and attributed to symbiont photosynthetic activity [*Eggins et al.*, 2004], yet neither of the species studied here harbor photosymbionts. Similar banding has been described in benthic species that have much higher Mg/Ca ratios than these planktonic foraminifera [*Erez*, 2003; *Bentov and Erez*, 2005]; these authors also conclude that the high Mg/Ca layer is primary calcite precipitated next to the organic membrane.

4.2.1. Environmental Controls

[19] The range in Mg/Ca observed here within a single test is similar to that reported previously [e.g., *Sadekov et*

al., 2005; *Anand and Elderfield*, 2005]. The question central to this and previous studies is what controls the variation in Mg/Ca? It is well known that planktonic foraminifera migrate vertically through the water column and add their gametogenic crust at depth in colder waters [e.g., *Orr*, 1967; *Rosenthal et al.*, 2000]. Given the close relationship between foraminiferal Mg/Ca and temperature [e.g., *Anand et al.*, 2003], this could result in variable Mg/Ca. However, the temperature of the water column at the PAP site when the foraminifera calcified (April–May) is well established and, over the depth range of these species, varies between 9.5 and 12.5°C (Figure 2). Using calibrations [*Anand et al.*, 2003] obtained from measurements of multiple foraminifera tests (no calibrations based on single tests, or individual components of single tests, are available), this corresponds to Mg/Ca values of ~0.9–1.2 mmol/mol, which is significantly less than the range recorded here (~0.4–3.6 mmol/mol (Figure 6)). Salinity also varies over the depth range of these species, but only by ~0.2 units which would have a negligible effect on Mg/Ca [e.g., *Kisakürek et al.*, 2008]. Meanwhile, $[CO_3^{2-}]$ varies between 130 and 190 μmol/L (Figure 2), but culturing studies of planktonic foraminiferal reveal that, for these values of $[CO_3^{2-}]$, there is no effect on foraminiferal Mg/Ca [e.g., *Russell et al.*, 2004].

[20] The B/Ca ratio of the innermost part of the test wall of *G. inflata* is ~20 μmol/mol higher than that recorded for the outer part; for *G. scitula* the difference is even greater (~40 μmol/mol) (Figure 6). *Yu et al.* [2007] have demonstrated that B/Ca of *G. inflata* varies both as a function of pH and also of temperature. pH measurements are not available for the PAP site, but can be estimated from measurements of pressure, temperature, salinity, phosphate, silicate, total alkalinity and TCO_2 from a nearby site [*Rommets*, 2003; *Rommets et al.*, 1991, 2003], together with the CO2sys macro [*Pierrot et al.*, 2006]. In this way, foraminiferal B/Ca is expected to vary between ~90 μmol/mol in surface waters and ~60 and ~40 μmol/mol at depths of 300 m and 1000 m, respectively. These values agree remarkably well with those measured across the test walls, raising the possibility that intratest variations in B/Ca are the result of changes in pH and temperature due to vertical migration of the foraminifera.

[21] Li is conservative in the oceans [*Stoffyn-Egli and Mackenzie*, 1984] so variations in foraminiferal Li/Ca cannot be attributed to changes in seawater Li/Ca. Temperature appears to regulate the Li/Ca ratio of inorganic calcite [*Marriott et al.*, 2004], but the size of this effect is small and acts in the wrong direction to explain the variation in the Li/Ca ratio between the innermost (>30 μmol/mol) and outermost (10 μmol/mol) calcite observed here. Furthermore,

studies of planktonic foraminifera indicate that the relationship between temperature and the Li/Ca ratio is weak [*Hathorne and James*, 2006; *Hall and Chan*, 2004]. Changes in seawater [CO_3^{2-}] must also be considered as *Lear and Rosenthal* [2006] have suggested that the Li/Ca ratio of benthic foraminiferal calcite falls by ∼10% as the degree of calcite saturation (ΔCO_3^{2-}, the difference between seawater [CO_3^{2-}] and [CO_3^{2-}] required for calcite to be at saturation) falls from 45 to 5 μmol kg^{-1}. At the PAP site, ΔCO_3^{2-} ranges from 80 to 130 μmol kg^{-1} over the depth range for calcification of *G. inflata* and *G. scitula*; if the relationship between Li/Ca and ΔCO_3^{2-} for benthic foraminifera holds for these species then Li/Ca would be expected to decrease by ∼13% through the shell wall which is far less than is measured here. Recently, *Bryan and Marchitto* [2008] observed a decrease of ∼20% in the Li/Ca of benthic foraminiferal calcite as ΔCO_3^{2-} increased from 50 to 150 μmol kg^{-1} in the Florida Straits. Again, if this effect is important for planktonic foraminiferal calcite, then it is too small and acts in the wrong direction to explain the intratest Li/Ca pattern that we observe here.

[22] Manganese and barium are classified as recycled elements in seawater, as their concentration is low in surface waters and increases with depth [e.g., *Bruland and Lohan*, 2003]. In this study, we find that the outer part of the test, which formed in deeper waters, has lower Mn/Ca and Ba/Ca than the inner part of the test so vertical migration cannot account for the intratest variation in these elements. Whether changes in Mn/Ca and Ba/Ca are effected by other variables is not clear from the literature, as studies of these trace elements are scarce.

[23] Sr/Ca ratios show little variability across the test walls of *G. scitula* and *G. inflata*. A temperature control on the Sr/Ca ratio of deeper dwelling *Globorotalia* species has been reported by *Elderfield et al.* [2000] and *Cléroux et al.* [2008], but if there is any temperature control on Sr/Ca for the species measured in this study then it is smaller than the external precision of the analyses (∼10% (Figure S2)).

[24] To summarize, the data that we present here seem to demonstrate that, with the exception of B/Ca, the intratest variation in Mg/Ca, Li/Ca, Mn/Ca and Ba/Ca of *G. scitula* and *G. inflata* is not primarily controlled by environmental parameters. Furthermore, because the tests were collected over a very short (2 week) time period, differences between the chemical composition of the individual tests are also unlikely to be due to differences in environmental parameters, such as temperature and salinity. For these reasons, this data set can provide crucial insight as to the biomineralization control on trace element/Ca ratios; such information may be lost in core top studies, because the individual tests will have grown during different seasons and years, stretching often up to thousands of years into the past.

4.2.2. Biomineralization Controls

[25] Foraminifera can regulate the trace element composition of their tests in a number of different ways. The aim here is to identify which of a number of different biomineralization processes can reproduce the sense and magnitude of the mixing relationships that we observe between Mg/Ca and Mn/Ca, Sr/Ca and Ba/Ca (Table 1 and Figure 7). Only the divalent cations are considered, because these are known to substitute for Ca^{2+} in the calcite lattice [*Reeder et al.*, 1999].

[26] First, we consider the effect of precipitation rate. A number of laboratory studies have shown that the partition coefficient, D_X, between element X in inorganic calcite and in solution varies as function of calcite precipitation rate [e.g., *Lorens*, 1981; *Tesoriero and Pankow*, 1996]. While the precipitation rate of foraminiferal calcite is thought to be slower (by a factor of 2 or more) than the precipitation rate of inorganic calcite [*Erez*, 2003], a precipitation rate control on the trace element composition of foraminiferal calcite is often implicated in the literature [e.g., *Hall and Chan*, 2004; *Russell et al.*, 2004]. The variation in D_X as a function of precipitation rate can be modeled in terms of ion mobility at the calcite-solution interface; this is a function only of ion size when the charge is the same [*Watson*, 2004]. Figure 8a shows the effect of changing precipitation rate on D_X; note that D_{Mg} is independent of precipitation rate [e.g., *Morse and Bender*, 1990], while the rate dependences of D_{Mn} and D_{Ba} act in opposite directions. This is in contrast to the trends shown in Figure 7, suggesting that precipitation rate is not responsible for the intratest variation in trace element/Ca ratios, at least for the divalent cations. Furthermore, changes in precipitation rate cannot explain the small variation observed in Sr/Ca relative to other trace elements.

[27] Second, it seems likely that the perforate foraminifera (which include *G. scitula* and *G. inflata*) incorporate Ca^{2+} and trace elements via intracellular vacuoles that serve as reservoirs for calcification [*Erez*, 2003]. The composition of the solution in the vacuoles is similar but not necessarily identical to seawater [*Elderfield et al.*, 1996; *Erez*, 2003] and trace elements are extracted from it during the biomineralization process. If this is the case, then the composition of the foraminiferal calcite changes as a function of the fraction of Ca^{2+} remaining in the reservoir. This can be modeled in terms of Rayleigh distillation [*Elderfield et al.*, 1996] and the results are shown in Figure 8b. One of the predictions of this model is that intratest heterogeneity will be large for ions that have $D_X > 1$ (Mn^{2+}) but small for ions that have $D_X < 1$ (Sr^{2+}, Ba^{2+}, Mg^{2+}). Our data indicate that this is true for Sr but not for Ba. The model also predicts that the relationship between D_X and the size of the Ca^{2+} reservoir for elements with $D_X > 1$ is opposite to that for elements with $D_X < 1$. Thus, Mn^{2+} and Ba^{2+} should show contrasting behavior (Figure 8b), but this is not what we observe in our data (Figure 7). In addition, it is difficult to reconcile the abrupt changes in the Mg/Ca ratio of the test (as revealed by EMP (Figure 3)) with the smooth, gradual nature of a distillation process.

[28] Finally, the incorporation of trace elements into foraminiferal calcite can be affected by changes in the structural form of the calcite [*Russell et al.*, 2004]. Figure 4 demonstrates that the structure of the calcite crystals that form the inner and outermost parts of the test wall are distinctly different and, in this connection, it is well documented that calcite growth hillocks have two types of vicinal faces with the positive faces incorporating trace elements in a way that is different from the negative faces [e.g., *Paquette and Reeder*, 1990, 1995; *Reeder*, 1996]. It is also recognized

that the proportional area of each of these faces can be altered by Mg incorporation [*Davis et al.*, 2004] and the presence of amino acids [*Orme et al.*, 2001]. The average

composition of the calcite (C_{av}) can be calculated in terms of the relative proportion of positive versus negative faces:

$$C_{av} = C_{+ve}P_{+ve} + C_{-ve}P_{-ve} \qquad (1)$$

where C_{+ve} and C_{-ve} are the trace element concentration of the positive and negative faces, respectively, taken from *Paquette and Reeder* [1990] and *Reeder* [1996], and P_{+ve} and P_{-ve} are the fractional proportion of positive and negative faces ($P_{+ve} + P_{-ve} = 1$). The results of this calculation are shown in Figure 8c. This model successfully accounts for the small variation in Sr/Ca, but the relationship between Mg/Ca and Ba/Ca is in the opposite sense to that which we observe (Figure 7). Moreover, while the model can reproduce the covariation between Mg/Ca and Mn/Ca shown in Figure 7, it accounts for <30% of the range of values that we measure. One complication, however, is that the crystal face preference of Mg can shift depending on whether calcite growth is diffusion or surface reaction limited [*Wasylenki et al.*, 2005]; this is not accounted for in the model presented here.

[29] Although this exercise is instructive, none of the biomineralization processes discussed above can, by themselves, account for intratest variations in the composition of calcite that we observe. Nevertheless, it is likely that trace element/Ca ratios are affected by more than one process, and there is a need to establish an integrated biomineralization model, as well as models for other biomineralization processes. Much more knowledge is required concerning the effect of precipitation rate on the crystal face preferences of various elements and the influence of specific organic molecules, known to be integral to foraminiferal calcite [*Robbins and Brew*, 1990; *Robbins and Donachy*, 1991], on crystal structure and trace element partitioning. Additionally, cellular ion transport also has the potential to alter the chemistry of foraminiferal calcite [e.g., *Gussone et al.*, 2003] but little is known about this process. What is clear, however, is that the Mg/Ca ratios that we have measured in this study imply that the Mg/Ca of the solution from which the foraminifera calcifies is at least an order of magnitude lower than the Mg/Ca ratio of seawater. How the foraminifera regulate the Mg/Ca ratio of the calcifying solution is still debated [*Bentov and Erez*, 2006], but changes in the solution Mg/Ca will likely impact the crystal size and orientation [*Kwak et al.*, 2005] suggesting that the foraminifera regulate the Mg/Ca ratio of the solution to control crystal growth. The difference in crystal structure between the inner and outer calcite (see Figure 4) could be the direct result of the difference in Mg/Ca between the inner and
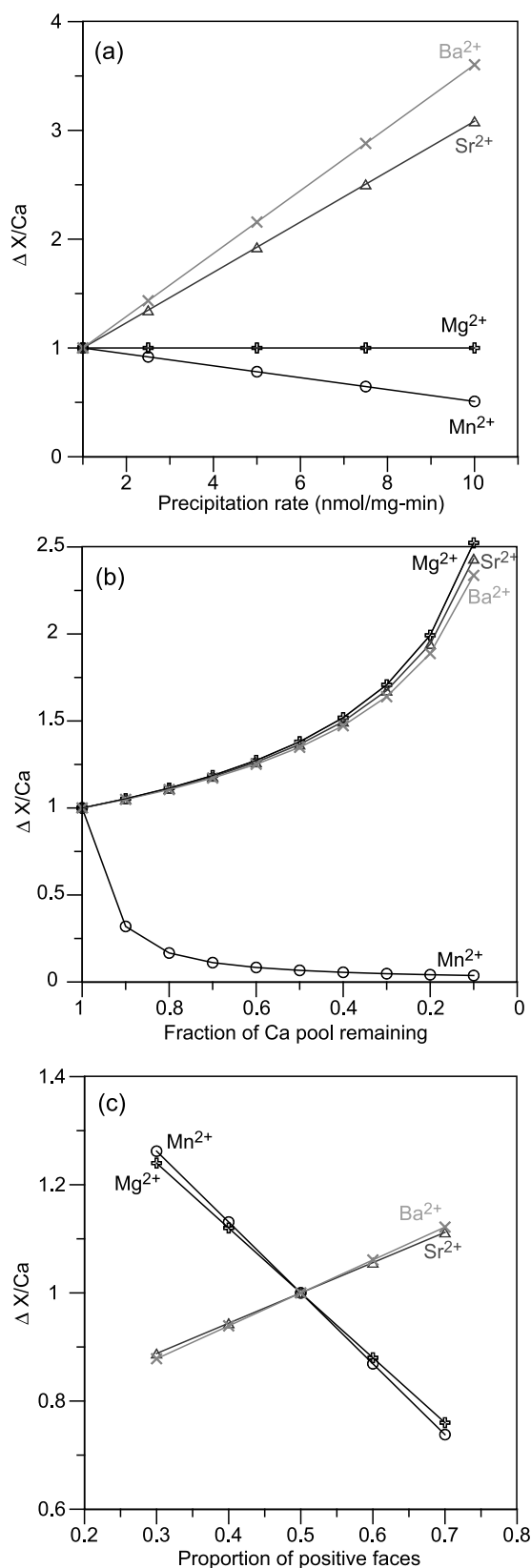
Figure 8. Graphs showing the variation in X/Ca ratio as a result of (a) changes in precipitation rate, (b) Rayleigh distillation of the calcifying solution, and (c) changes in calcite structure. For Figure 8a, data are from *Lorens* [1981] for D_{Mn} and from *Tesoriero and Pankow* [1996] for D_{Sr} and D_{Ba}. For Figure 8b equation (vii) from *Elderfield et al.* [1996] was used. Note that X/Ca is reported relative to the initial value as the absolute value is dependent on the boundary conditions employed by each model.
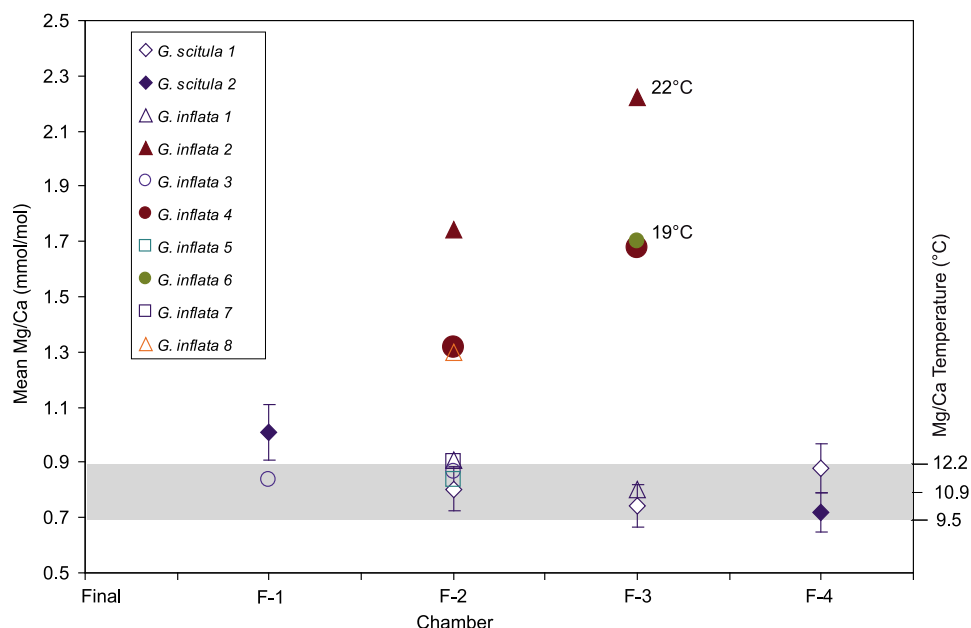
Figure 9. Average Mg/Ca ratio of different chambers of *G. scitula* and *G. inflata* tests. Error bars (only shown for *G. scitula*) are the external error (1σ) of a 60 s analysis of a coral standard pellet (JCp-1). Mg/Ca temperature is derived from the bulk *G. inflata* calibration published by *Anand et al.* [2003]. Smaller *G. inflata* tests with 3.5 chambers in the final whorl are shown by the solid circles and triangles.

outer calcite. This implies that D_{Mg} is primarily a function of solution Mg/Ca, as regulated by the organism, and not temperature. This is a departure from the model of *Bentov and Erez* [2006] in which test Mg/Ca is defined by the proportion of high Mg (primary) calcite to low Mg (secondary) calcite, which in turn is regulated by temperature, and it suggests that a detailed examination of the possible physiological impacts on the foraminiferal Mg/Ca paleothermometer is required.

4.3. Implications for Paleoceanographic Studies

[30] Even though the intratest variation in trace element/Ca ratios is large, the average Mg/Ca ratio of an individual analysis gives an Mg/Ca temperature that generally matches the water temperature measured at the PAP site (Figure 9). However, the average Mg/Ca ratio of smaller *G. inflata* tests (mean diameter 438 μm) is ~1 mmol/mol higher than that of the larger tests (mean diameter 538 μm), giving Mg/Ca temperatures that greatly exceed those measured in the water column (Figure 9). This difference between these morphologically distinct tests is much greater than that previously observed for different *G. ruber* morphotypes [*Steinke et al.*, 2005]. We also note that the proportion of inner to outer calcite varies between chambers in these smaller tests and their test walls are generally thinner (note the reduced ablation time (Figure 6)). Additionally, the outer part of the smaller tests has higher Mg/Ca than the outer part of the larger tests. These small tests are morphologically distinct in that they have between 3 and 3.5 chambers in the final whorl, as opposed to 4 (Figure 10). These different morphotypes have previously been documented in fossilized tests preserved in marine sediments [*Loubere and Chellappa*, 2008], but note that in this study, the tests were collected from the water column during a short (2 week) time period, so the large difference in Mg/Ca between these two populations (large versus small) is difficult to explain in terms of environmental parameters. Genetic studies published to date indicate only one genotype of *G. inflata*
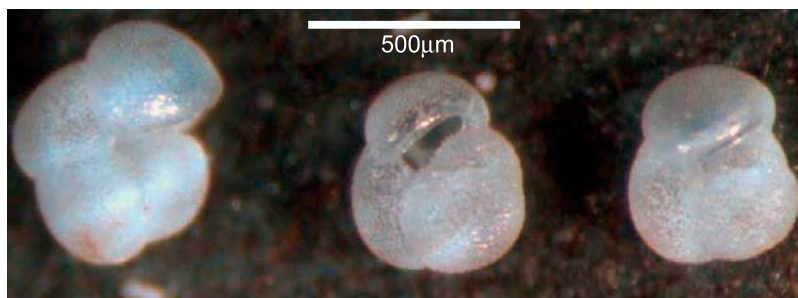

Figure 10. *G. inflata* tests with 4 chambers (left) and 3.5 chambers (middle and right) in the final whorl.

although distinct genetic populations cannot be ruled out [*Darling and Wade*, 2008]. The location of the trap and the size of the tests preclude lateral transport of >100 km, so we must conclude that there is an extreme physiological influence on the shell morphology, structure and Mg/Ca ratio. The size of *G. inflata* shells seems to vary with proloculus size and ontogenetic growth stage [*Wei et al.*, 1992] which, in turn, may depend on the availability of food on time scales of a few days, possibly because of storms and eddies (section 2.2). This highlights the need for extra care when selecting tests for paleoceanographic studies; specifically, the $3-3.5$ chambered *G. inflata* morphotype should be separated from the 4 chamber morphotype.

[31] Finally, calcite with higher Mg/Ca is more soluble [e.g., *Davis et al.*, 2000] and there is a well-documented differential dissolution effect on foraminiferal Mg/Ca ratios [e.g., *Benway et al.*, 2003]. The pattern of intratest Li/Ca, B/Ca, Mn/Ca and Ba/Ca heterogeneity is similar to that of Mg/Ca, so our data raise the possibility that these elements may also be affected by differential dissolution beneath the calcite lysocline.

5.   Conclusions

[32] The pattern of the intratest variation in Li, B, Mn, and Ba in *G. inflata* and *G. scitula* tests from a sediment trap in the northeast Atlantic is similar to that observed for Mg/Ca. The inner part of the test wall has the highest trace element/Ca ratios, while the outer part of the wall, which likely represents the gametogenic crust, has lower trace element/Ca ratios. By contrast, there is little variation (<10%) in the Sr/Ca ratio within individual tests. Comparison with water column parameters, including temperature, salinity and $[CO_3^{2-}]$, indicates that (with the exception of B/Ca) the variation in trace element/Ca is not due to vertical migration of the foraminifera, but rather it must be the result of biomineralization processes. However, models of (1) calcite precipitation rate, (2) Rayleigh distillation of the calcifying reservoir and (3) crystal structure are unable individually to explain the patterns of the intratest element/Ca variation that we have observed.

[33] Despite large intratest variations in Mg/Ca ratios, the mean value of an individual analysis produces a Mg/Ca temperature (based on calibrations using bulk foraminifera) that accurately reflects (in most cases) that which is measured in the water column in which the test grew. The exception is smaller *G. inflata* tests. These tests are morphologically different in that they have only $3-3.5$ chambers in their final whorl (as opposed to 4), they also have higher Mg/Ca (by ~1 mmol/mol), yet they coexist with the larger *G. inflata* tests which have Mg/Ca ratios that give temperatures similar to those measured in the water column. The smaller tests should therefore be separated from their larger (4 chambered) counterparts in paleoceanographic studies.

References

Addadi, L., S. Raz, and S. Weiner (2003), Taking advantage of disorder: Amorphous calcium carbonate and its roles in biomineralization, *Adv. Mater.*, *15*, 959–970, doi:10.1002/adma.200300381.

Anand, P., and H. Elderfield (2005), Variability of Mg/Ca and Sr/Ca between and within the planktonic foraminifers *Globigerina bulloides* and *Globorotalia truncatulinoides*, *Geochem. Geophys. Geosyst.*, *6*, Q11D15, doi:10.1029/2004GC000811.

Anand, P., H. Elderfield, and M. H. Conte (2003), Calibration of Mg/Ca thermometry in planktonic foraminifera from a sediment trap time series, *Paleoceanography*, *18*(2), 1050, doi:10.1029/2002PA000846.

Barker, S., M. Greaves, and H. Elderfield (2003), A study of cleaning procedures used for foraminiferal Mg/Ca paleothermometry, *Geochem. Geophys. Geosyst.*, *4*(9), 8407, doi:10.1029/2003GC000559.

Bé, A. W. H. (1980), Gametogenic calcification in a spinose planktonic foraminifer, *Globigerinoides sacculifer* (Brady), *Mar. Micropaleontol.*, *5*, 283–310, doi:10.1016/0377-8398(80)90014-6.

Bé, A. W. H., C. Hemleben, O. R. Anderson, and M. Spindler (1979), Chamber formation in planktonic foraminifera, *Micropaleontology*, *25*, 294–307, doi:10.2307/1485304.

Bentov, S., and J. Erez (2005), Novel observations on biomineralization processes in foraminifera and implications for Mg/Ca ratio in the shells, *Geology*, *33*, 841–844, doi:10.1130/G21800.1.

Bentov, S., and J. Erez (2006), Impact of biomineralization processes on the Mg content of foraminiferal shells: A biological perspective,

Geochem. Geophys. Geosyst., *7*, Q01P08, doi:10.1029/2005GC001015.

Benway, H. M., B. A. Haley, G. P. Klinkhammer, and A. C. Mix (2003), Adaptation of a flow-through leaching procedure for Mg/Ca paleothermometry, *Geochem. Geophys. Geosyst.*, *4*(2), 8403, doi:10.1029/2002GC000312.

Bower, A. S., B. Le Cann, T. Rossby, W. Zenk, J. Gould, K. Speer, P. L. Richardson, M. D. Prater, and H.-M. Zhang (2002), Directly measured mid-depth circulation in the northeastern North Atlantic Ocean, *Nature*, *419*, 603–607, doi:10.1038/nature01078.

Brown, S. J., and H. Elderfield (1996), Variations in Mg/Ca and Sr/Ca ratios of planktonic foraminifera caused by postdepositional dissolution: Evidence of shallow Mg-dependent dissolution, *Paleoceanography*, *11*, 543–551, doi:10.1029/96PA01491.

Bruland, K. W., and M. C. Lohan (2003), Controls of trace metals in seawater, in *The Oceans and Marine Geochemistry*, edited by H. Elderfield, pp. 23–47, Elsevier, Oxford, U. K.

Bryan, S. P., and T. M. Marchitto (2008), Mg/Ca-temperature proxy in benthic foraminifera: New calibrations from the Florida Straits and a hypothesis regarding Mg/Li, *Paleoceanography*, *23*, PA2220, doi:10.1029/2007PA001553.

Caron, D. A., O. R. Anderson, J. L. Lindsey, W. W. J. Faber, and E. Lim (1990), Effects of gametogenesis on test structure and dissolution of some spinose planktonic foraminifera and implications for test preservation, *Mar. Micropaleontol.*, *16*, 93–116, doi:10.1016/0377-8398(90)90031-G.

Chiessi, C. M., S. Ulrich, S. Mulitza, J. Pätzold, and G. Wefer (2007), Signature of the Brazil-Malvinas Confluence (Argentine Basin) in the isotopic composition of planktonic foraminifera from surface sediments, *Mar. Micropaleontol.*, *64*, 52–66, doi:10.1016/j.marmicro.2007.02.002.

Cléroux, C., E. Cortijo, J.-C. Duplessy, and R. Zahn (2007), Deep-dwelling foraminifera as thermocline temperature recorders, *Geochem. Geophys. Geosyst.*, *8*, Q04N11, doi:10.1029/2006GC001474.

Cléroux, C., E. Cortijo, P. Anand, L. Labeyrie, F. Bassinot, N. Caillon, and J.-C. Duplessy (2008), Mg/Ca and Sr/Ca ratios in planktonic foraminifera: Proxies for upper water column temperature reconstruction, *Paleoceanography*, *23*, PA3214, doi:10.1029/2007PA001505.

Darling, K. F., and C. M. Wade (2008), The genetic diversity of planktic foraminifera and the global distribution of ribosomal RNA genotypes, *Mar. Micropaleontol.*, *67*, 216–238, doi:10.1016/j.marmicro.2008.01.009.

Davis, K. J., P. M. Dove, and J. J. De Yoreo (2000), The role of Mg^{2+} as an impurity in calcite growth, *Science*, *290*, 1134–1137, doi:10.1126/science.290.5494.1134.

Davis, K. J., P. M. Dove, L. E. Wasylenki, and J. J. De Yoreo (2004), Morphological consequences of differential Mg^{2+} incorporation at structurally distinct steps on calcite, *Am. Mineral.*, *89*, 714–720.

Eggins, S., P. De Deckker, and J. Marshall (2003), Mg/Ca variation in planktonic foraminifera tests: Implications for reconstructing palaeoseawater temperature and habitat migration,

Earth Planet. Sci. Lett., *212*, 291–306, doi:10.1016/S0012-821X(03)00283-8.

Eggins, S. M., A. Sadekov, and P. De Deckker (2004), Modulation and daily banding of Mg/Ca in *Orbulina universa* tests by symbiont photosynthesis and respiration: A complication for seawater thermometry?, *Earth Planet. Sci. Lett.*, *225*, 411–419, doi:10.1016/j.epsl.2004.06.019.

Elderfield, H., and R. E. M. Rickaby (2000), Oceanic Cd/P ratio and nutrient utilization in the glacial Southern Ocean, *Nature*, *405*, 305–310, doi:10.1038/35012507.

Elderfield, H., C. J. Bertram, and J. Erez (1996), A biomineralization model for the incorporation of trace elements into foraminiferal calcium carbonate, *Earth Planet. Sci. Lett.*, *142*, 409–423, doi:10.1016/0012-821X(96)00105-7.

Elderfield, H., M. Cooper, and G. Ganssen (2000), Sr/Ca in multiple species of planktonic foraminifera: Implications for reconstructions of seawater Sr/Ca, *Geochem. Geophys. Geosyst.*, *1*(11), 1017, doi:10.1029/1999GC000031.

Elderfield, H., M. Vautravers, and M. Cooper (2002), The relationship between shell size and Mg/Ca, Sr/Ca, δ^{18}O, and δ^{13}C of species of planktonic foraminifera, *Geochem. Geophys. Geosyst.*, *3*(8), 1052, doi:10.1029/2001GC000194.

Erez, J. (2003), The source of ions for biomineralization in foraminifera and their implications for paleoceanographic proxies, *Rev. Mineral. Geochem.*, *54*, 115–149, doi:10.2113/0540115.

Erez, J., and S. Honjo (1981), Comparison of isotopic composition of planktonic foraminifera in plankton tows, sediment traps and sediments, *Palaeogeogr. Palaeoclimatol. Palaeoecol.*, *33*, 129–156.

Fairbanks, R. G., P. H. Wiebe, and A. W. H. Bé (1980), Vertical distribution and isotopic composition of living planktonic foraminifera in the western North Atlantic, *Science*, *207*, 61–63, doi:10.1126/science.207.4426.61.

Fratantoni, D. M. (2001), North Atlantic surface circulation during the 1990's observed with satellite-tracked drifters, *J. Geophys. Res.*, *106*, 22,067–22,093, doi:10.1029/2000JC000730.

Gehlen, M., F. Bassinot, L. Beck, and H. Khodja (2004), Trace element cartography of Globigerinoides ruber shells using particle-induced X-ray emission, *Geochem. Geophys. Geosyst.*, *5*, Q12D12, doi:10.1029/2004GC000822.

Gussone, N., A. Eisenhauer, A. Heuser, M. Dietzel, B. Bock, F. Böhm, H. J. Spero, D. W. Lea, J. Bijma, and T. F. Nägler (2003), Model for kinetic effects on calcium isotope fractionation (δ^{44}Ca) in inorganic aragonite and cultured planktonic foraminifera, *Geochim. Cosmochim. Acta*, *67*, 1375–1382, doi:10.1016/S0016-7037(02)01296-6.

Hall, J. M., and L.-H. Chan (2004), Li/Ca in multiple species of benthic and planktonic foraminifera: Thermocline, latitudinal, and glacial-interglacial variation, *Geochim. Cosmochim. Acta*, *68*, 529–545, doi:10.1016/S0016-7037(03)00451-4.

Harvey, J., and S. Glynn (1985), Water mass structure and transport in the Tourbillon eddy, *Deep Sea Res., Part A*, *32*, 675–695, doi:10.1016/0198-0149(85)90072-X.

Hathorne, E. C., and R. H. James (2006), Temporal record of lithium in seawater: A tracer for silicate weathering?, *Earth Planet. Sci. Lett.*, *246*, 393–406, doi:10.1016/j.epsl.2006.04.020.

Hathorne, E. C., O. Alard, R. H. James, and N. W. Rogers (2003), Determination of intratest variability of trace elements in foraminifera by laser ablation inductively coupled plasma-mass spectrometry, *Geochem. Geophys. Geosyst.*, *4*(12), 8408, doi:10.1029/2003GC000539.

Hathorne, E. C., R. H. James, P. Savage, and O. Alard (2008), Physical and chemical characteristics of particles produced by laser ablation of biogenic calcium carbonate, *J. Anal. At. Spectrom.*, *23*, 240–243, doi:10.1039/b706727e.

Hemleben, C., M. Spindler, and O. R. Anderson (1989), *Modern Planktonic Foraminifera*, Springer, New York.

Heywood, K. J., E. L. McDonagh, and M. A. White (1994), Eddy kinetic energy of the North Atlantic subpolar gyre from satellite altimetry, *J. Geophys. Res.*, *99*, 22,525–22,539, doi:10.1029/94JC01740.

Honjo, S., and K. W. Doherty (1988), Large aperture time series sediment traps: Design objectives, construction and applications, *Deep Sea Res., Part A*, *35*, 133–149, doi:10.1016/0198-0149(88)90062-3.

Itou, M., T. Ono, T. Oba, and S. Noriki (2001), Isotopic composition and morphology of living *Globorotalia scitula*: A new proxy of subintermediate ocean carbonate chemistry?, *Mar. Micropaleontol.*, *42*, 189–210, doi:10.1016/S0377-8398(01)00015-9.

Kisakürek, B., A. Eisenhauer, F. Böhm, D. Garbe-Schönberg, and J. Erez (2008), Controls on shell Mg/Ca and Sr/Ca in cultured planktonic foraminiferan, *Globigerinoides ruber* (white), *Earth Planet. Sci. Lett.*, *273*, 260–269, doi:10.1016/j.epsl.2008.06.026.

Kunioka, D., K. Shirai, N. Takahata, Y. Sano, T. Toyofuku, and Y. Ujiie (2006), Microdistribution of Mg/Ca, Sr/Ca, and Ba/Ca ratios in *Pulleniatina obliquiloculata* test by using a NanoSIMS: Implication for the vital effect mechanism, *Geochem. Geophys. Geosyst.*, *7*, Q12P20, doi:10.1029/2006GC001280.

Kwak, S.-Y., E. DiMasi, Y.-J. Han, J. Aizenberg, and I. Kuzmenko (2005), Orientation and Mg incorporation of calcite grown on functionalized self-assembled monolayers: A synchrotron X-ray study, *Cryst. Growth Des.*, *5*, 2139–2145, doi:10.1021/cg050164x.

Lampitt, R. S., P. P. Newton, T. D. Jickells, J. Thomson, and P. King (2000), Near-bottom particle flux in the abyssal northeast Atlantic, *Deep Sea Res., Part II*, *47*, 2051–2071, doi:10.1016/S0967-0645(00)00016-3.

Lampitt, R. S., B. J. Bett, K. Kiriakoulakis, E. E. Popova, O. Ragueneau, A. Vangriesheim, and G. A. Wolff (2001), Material supply to the abyssal seafloor in the northeast Atlantic, *Prog. Oceanogr.*, *50*, 27–63, doi:10.1016/S0079-6611(01)00047-7.

Lea, D. W., T. A. Mashiotta, and H. J. Spero (1999), Controls on magnesium and strontium uptake in planktonic foraminifera determined by live culturing, *Geochim. Cosmochim. Acta*, *63*, 2369–2379, doi:10.1016/S0016-7037(99)00197-0.

Lear, C. H., and Y. Rosenthal (2006), Benthic foraminiferal Li/Ca: Insights into Cenozoic seawater carbonate saturation state, *Geology*, *34*, 985–988, doi:10.1130/G22792A.1.

Lear, C. H., H. Elderfield, and P. A. Wilson (2000), Cenozoic deep-sea temperatures and global ice volumes from Mg/Ca in benthic foraminiferal calcite, *Science*, *287*, 269–272, doi:10.1126/science.287.5451.269.

Lochte, K., and O. Pfannkuche (1987), Cyclonic cold-core eddy in the eastern North Atlantic. INutrients, I., phytoplankton and bacterioplankton, *Mar. Ecol. Prog. Ser.*, *39*, 153–164, doi:10.3354/meps039153.

Lončarić, N., F. J. C. Peeters, D. Kroon, and G.-J. A. Brummer (2006), Oxygen isotope ecology of recent planktic foraminifera at the central Walvis Ridge (SE Atlantic), *Paleoceanography*, *21*, PA3009, doi:10.1029/2005PA001207.

Lorens, R. B. (1981), Sr, Cd, Mn and Co distribution coefficients in calcite as a function of calcite precipitation rate, *Geochim. Cosmochim. Acta*, *45*, 553–561, doi:10.1016/0016-7037(81)90188-5.

Loubere, P., and R. Chellappa (2008), Carbonate preservation in marine sediments: Mid to higher latitude quantitative proxies, *Paleoceanography*, *23*, PA1209, doi:10.1029/2007PA001470.

Marriott, C. S., G. M. Henderson, N. S. Belshaw, and A. W. Tudhope (2004), Temperature dependence of δ^7Li, δ^{44}Ca and Li/Ca during growth of calcium carbonate, *Earth Planet. Sci. Lett.*, *222*, 615–624, doi:10.1016/j.epsl.2004.02.031.

McConnell, M. C., and R. C. Thunell (2005), Calibration of the planktonic foraminiferal Mg/Ca paleothermometer: Sediment trap results from the Guaymas Basin, Gulf of California, *Paleoceanography*, *20*, PA2016, doi:10.1029/2004PA001077.

McGillicuddy, D. J. J., et al. (2007), Eddy/wind interactions stimulate extraordinary mid-ocean plankton blooms, *Science*, *316*, 1021–1026, doi:10.1126/science.1136256.

Mittelstaedt, E. (1987), Cyclonic cold-core eddy in the eastern North Atlantic. I. Physical description, *Mar. Ecol. Prog. Ser.*, *39*, 145–152, doi:10.3354/meps039145.

Morse, J. W., and M. L. Bender (1990), Partition coefficients in calcite: Examination of factors influencing the validity of experimental results and their application to natural systems, *Chem. Geol.*, *82*, 265–277, doi:10.1016/0009-2541(90)90085-L.

Newton, P. P., R. S. Lampitt, T. D. Jickells, P. King, and C. Boutle (1994), Temporal and spatial variability of biogenic particle fluxes during the JGOFS northeast Atlantic process studies at 47°N, 20°W, *Deep Sea Res., Part I*, *41*, 1617–1642, doi:10.1016/0967-0637(94)90065-5.

Ni, Y., G. L. Foster, T. Bailey, T. Elliott, D. N. Schmidt, P. Pearson, B. Haley, and C. Coath (2007), A core top assessment of proxies for the ocean carbonate system in surface-dwelling foraminifers, *Paleoceanography*, *22*, PA3212, doi:10.1029/2006PA001337.

Nürnberg, D., J. Bijma, and C. Hemleben (1996), Assessing the reliability of magnesium in foraminiferal calcite as a proxy for water mass temperatures, *Geochim. Cosmochim. Acta*, *60*, 803–814, doi:10.1016/0016-7037(95)00446-7.

Orme, C. A., A. Noy, A. Wierzbicki, M. T. McBride, M. Grantham, H. H. Teng, P. M. Dove, and J. J. De Yoreo (2001), Formation of chiral morphologies through selective binding of amino acids to calcite surface steps, *Nature*, *411*, 775–779, doi:10.1038/35081034.

Orr, W. N. (1967), Secondary calcification in the foraminiferal genus Globorotalia, *Science*, *157*, 1554–1555, doi:10.1126/science.157.3796.1554.

Ortiz, J. D., A. C. Mix, W. Rugh, J. M. Watkins, and R. W. Collier (1996), Deep-dwelling planktonic foraminifera of the northeastern Pacific Ocean reveal environmental control of oxygen and carbon isotopic disequilibria, *Geochim. Cosmochim. Acta*, *60*, 4509–4523, doi:10.1016/S0016-7037(96)00256-6.

Paquette, J., and R. J. Reeder (1990), New type of compositional zoning in calcite: Insights into crystal-growth mechanisms, *Geology*, *18*, 1244–1247, doi:10.1130/0091-7613(1990)018<1244:NTOCZI>2.3.CO;2.

Paquette, J., and R. J. Reeder (1995), Relationship between surface structure, growth mechanism,

and trace element incorporation in calcite, *Geochim. Cosmochim. Acta*, *59*, 735–749, doi:10.1016/0016-7037(95)00004-J.

Pierrot, D., E. Lewis, and D. W. R. Wallace (2006), MS Excel program developed for CO_2 system calculations, *ORNL/CDIAC-105a*, Carbon Dioxide Inf. Anal. Cent., Oak Ridge Natl. Lab., U.S. Dep. of Energy, Oak Ridge, Tenn.

Pingree, R. D. (1993), Flow of surface waters to the west of the British isles and in the Bay of Biscay, *Deep Sea Res., Part II*, *40*, 369–388, doi:10.1016/0967-0645(93)90022-F.

Pingree, R. D., and B. Le Cann (1991), Drifting buoy in the field of flow of two eddies on East Thulean Rise (northeast Atlantic), *J. Geophys. Res.*, *96*, 16,759–16,777, doi:10.1029/91JC01451.

Reeder, R. J. (1996), Interaction of divalent cobalt, zinc, cadmium, and barium with the calcite surface during layer growth, *Geochim. Cosmochim. Acta*, *60*, 1543–1552, doi:10.1016/0016-7037(96)00034-8.

Reeder, R. J., G. M. Lamble, and P. A. Northrup (1999), XAFS study of the coordination and local relaxation around Co^{2+}, Zn^{2+}, Pb^{2+}, and Ba^{2+} trace elements in calcite, *Am. Mineral.*, *84*, 1049–1060.

Robbins, L. L., and K. Brew (1990), Proteins from the organic matrix of core-top and fossil planktonic foraminifera, *Geochim. Cosmochim. Acta*, *54*, 2285–2292, doi:10.1016/0016-7037(90)90052-M.

Robbins, L. L., and J. E. Donachy (1991), Mineral regulating proteins from fossil planktonic foraminifera, in *Surface Reactive Peptides and Polymers: Discovery and Commercialization*, edited by C. S. Sikes and A. P. Wheeler, pp. 139–148, Am. Chem. Soc., Washington, D. C.

Robinson, A. R., et al. (1993), Mesoscale and upper ocean variabilities during the 1989 JGOFS bloom study, *Deep Sea Res., Part II*, *40*, 9–35, doi:10.1016/0967-0645(93)90004-7.

Rommets, J. (2003), Biogeochemical data from bottle station NAPP90-1_49-4, doi:10.1594/PANGAEA.94150, PANGAEA, Bremen, Germany.

Rommets, J., R. Dapper, and H. G. Fransz (1991), JGOFS North Atlantic R. V. *Tyro* Leg 3 of the cruise in 1990: Upper ocean processes, *Data Rep. 1991-1*, 44 pp., Neth. Inst. for Sea Res., Texel, Netherlands.

Rommets, J., K. Bakker, I. Flameling, S. Ober, M. H. C. Stoll, and S. Wijma (2003), Physical oceanography measured on water bottle samples at station NAPP90-1_49-1, doi:10.1594/PANGAEA.93997, PANGAEA, Bremen, Germany.

Rosenthal, Y., M. P. Field, and R. M. Sherrell (1999), Precise determination of element/calcium ratios in calcareous samples using sector field inductively coupled plasma mass spectrometry, *Anal. Chem.*, *71*, 3248–3253, doi:10.1021/ac981410x.

Rosenthal, Y., G. P. Lohmann, K. C. Lohmann, and R. M. Sherrell (2000), Incorporation and preservation of Mg in *Globigerinoides sacculifer*: Implications for reconstructing the temperature and $^{18}O/^{16}O$ of seawater, *Paleoceanography*, *15*, 135–145, doi:10.1029/1999PA000415.

Russell, A. D., B. Hönisch, H. J. Spero, and D. W. Lea (2004), Effects of seawater carbonate ion concentration and temperature on shell U, Mg, and Sr in cultured planktonic foraminifera, *Geochim. Cosmochim. Acta*, *68*, 4347–4361, doi:10.1016/j.gca.2004.03.013.

Sadekov, A. Y., S. M. Eggins, and P. De Deckker (2005), Characterization of Mg/Ca distributions in planktonic foraminifera species by electron microprobe mapping, *Geochem. Geophys. Geosyst.*, *6*, Q12P06, doi:10.1029/2005GC000973.

Sadekov, A., S. M. Eggins, P. De Deckker, and D. Kroon (2008), Uncertainties in seawater thermometry deriving from intratest and intertest Mg/Ca variability in *Globigerinoides ruber*, *Paleoceanography*, *23*, PA1215, doi:10.1029/2007PA001452.

Schauer, U. (1989), A deep saline cyclonic eddy in the West European Basin, *Deep Sea Res., Part A*, *36*, 1549–1565, doi:10.1016/0198-0149(89)90057-5.

Schiebel, R., B. Hiller, and C. Hemleben (1995), Impacts of storms on recent planktic foraminiferal test production and $CaCO_3$ flux in the North Atlantic 47°N, 20°W (JGOFS), *Mar. Micropaleontol.*, *26*, 115–129, doi:10.1016/0377-8398(95)00035-6.

Shoosmith, D. R., P. L. Richardson, A. S. Bower, and H. T. Rossby (2005), Discrete eddies in the northern North Atlantic as observed by looping RAFOS floats, *Deep Sea Res., Part II*, *52*, 627–650, doi:10.1016/j.dsr2.2004.12.011.

Siegel, D. A., and W. G. Deuser (1997), Trajectories of sinking particles in the Sargasso Sea: Modelling of statistical funnels above deep-ocean sediment traps, *Deep Sea Res., Part II*, *44*, 1519–1541, doi:10.1016/S0967-0637(97)00028-9.

Stammer, D., C. Wunsch, and K. Ueyoshi (2006), Temporal changes in ocean eddy transports, *J. Phys. Oceanogr.*, *36*, 543–550, doi:10.1175/JPO2858.1.

Steinke, S., H.-Y. Chiu, P.-S. Yu, C.-C. Shen, L. Löwemark, H.-S. Mii, and M.-T. Chen (2005), Mg/Ca ratios of two *Globigerinoides ruber* (white) morphotypes: Implications for reconstructing past tropical/subtropical surface water conditions, *Geochem. Geophys. Geosyst.*, *6*, Q11005, doi:10.1029/2005GC000926.

Stoffyn-Egli, P., and F. T. Mackenzie (1984), Mass balance of dissolved lithium in the oceans, *Geochim. Cosmochim. Acta*, *48*, 859–872, doi:10.1016/0016-7037(84)90107-8.

Tachikawa, K., S. Sépulcre, T. Toyofuku, and E. Bard (2008), Assessing influence of diagenetic carbonate dissolution on planktonic foraminiferal Mg/Ca in the southeastern Arabian Sea over the past 450 ka: Comparison between *Globigerinoides ruber* and *Globigerinoides sacculifer*, *Geochem. Geophys. Geosyst.*, *9*, Q04037, doi:10.1029/2007GC001904.

Takahashi, K., and A. W. H. Bé (1984), Planktonic foraminifera: Factors controlling sinking speeds, *Deep Sea Res., Part A*, *31*, 1477–1500, doi:10.1016/0198-0149(84)90083-9.

Tesoriero, A. J., and J. F. Pankow (1996), Solid solution partitioning of Sr^{2+}, Ba^{2+}, and Cd^{2+} to calcite, *Geochim. Cosmochim. Acta*, *60*, 1053–1063, doi:10.1016/0016-7037(95)00449-1.

Wasylenki, L. E., P. M. Dove, and J. J. De Yoreo (2005), Effects of temperature and transport conditions on calcite growth in the presence of Mg^{2+}: Implications for paleothermometry, *Geochim. Cosmochim. Acta*, *69*, 4227–4236, doi:10.1016/j.gca.2005.04.006.

Watson, E. B. (2004), A conceptual model for near-surface kinetic controls on the trace-element and stable isotope composition of abiogenic calcite crystals, *Geochim. Cosmochim. Acta*, *68*, 1473–1488, doi:10.1016/j.gca.2003.10.003.

Wei, K.-Y., Z.-W. Zhang, and C. Wray (1992), Shell ontogeny of Globorotalia inflata: Growth dynamics and ontogenetic stages, *J. Foraminiferal Res.*, *22*, 318–327.

Wilke, I., T. Bickert, and F. J. C. Peeters (2006), The influence of seawater carbonate ion concentration $[CO_3^-]$ on the stable carbon isotope composition of the planktic foraminifera species *Globorotalia inflata*, *Mar. Micropaleontol.*, *58*, 243–258, doi:10.1016/j.marmicro.2005.11.005.

Woodward, E. M. S., and A. P. Rees (2001), Nutrient distributions in an anticyclonic eddy in the northeast Atlantic Ocean, with reference to nanomolar ammonium concentrations, *Deep Sea Res., Part II*, *48*, 775–793, doi:10.1016/S0967-0645(00)00097-7.

Yu, J., H. Elderfield, and B. Hönisch (2007), B/Ca in planktonic foraminifera as a proxy for surface seawater pH, *Paleoceanography*, *22*, PA2202, doi:10.1029/2006PA001347.

─────────────────

E. C. Hathorne, Leibniz Institute of Marine Sciences at University of Kiel (IFM-GEOMAR), Wischhofstrasse 1-3, D-24148 Kiel, Germany. (ehathorne@marum.de)

R. H. James and R. S. Lampitt, National Oceanography Centre, Southampton SO14 3ZH, UK.